Layered mantle flow beneath the NE Asia from inversion of surface wave dispersion using rj-MCMC method

Zhao Yanzhe[1, 2], Guo Zhen[2], Wang Yanbin[1] and Fan Xingli[2]*

1 Department of Geophysics, School of Earth and Space Sciences, Peking University, Beijing 100871, China

2 Department of Ocean Science and Engineering, Southern University of Science and Technology, Shenzhen 518055, China

EGU2021 Apr. 29th, 2021

Background

- Geological background

  - **Trench-arc-backarc features :**

➢ **Volcanism**: Arc volcanoes and **Intraplate volcanoes**

➢ **Extensional Basins**, e.g. Songliao Basin, Bohaiwan Basin etc.

➢ **Marginal sea**: Sea of Japan

➢ **Large fault zone**: Tan-Lu Fault Zone

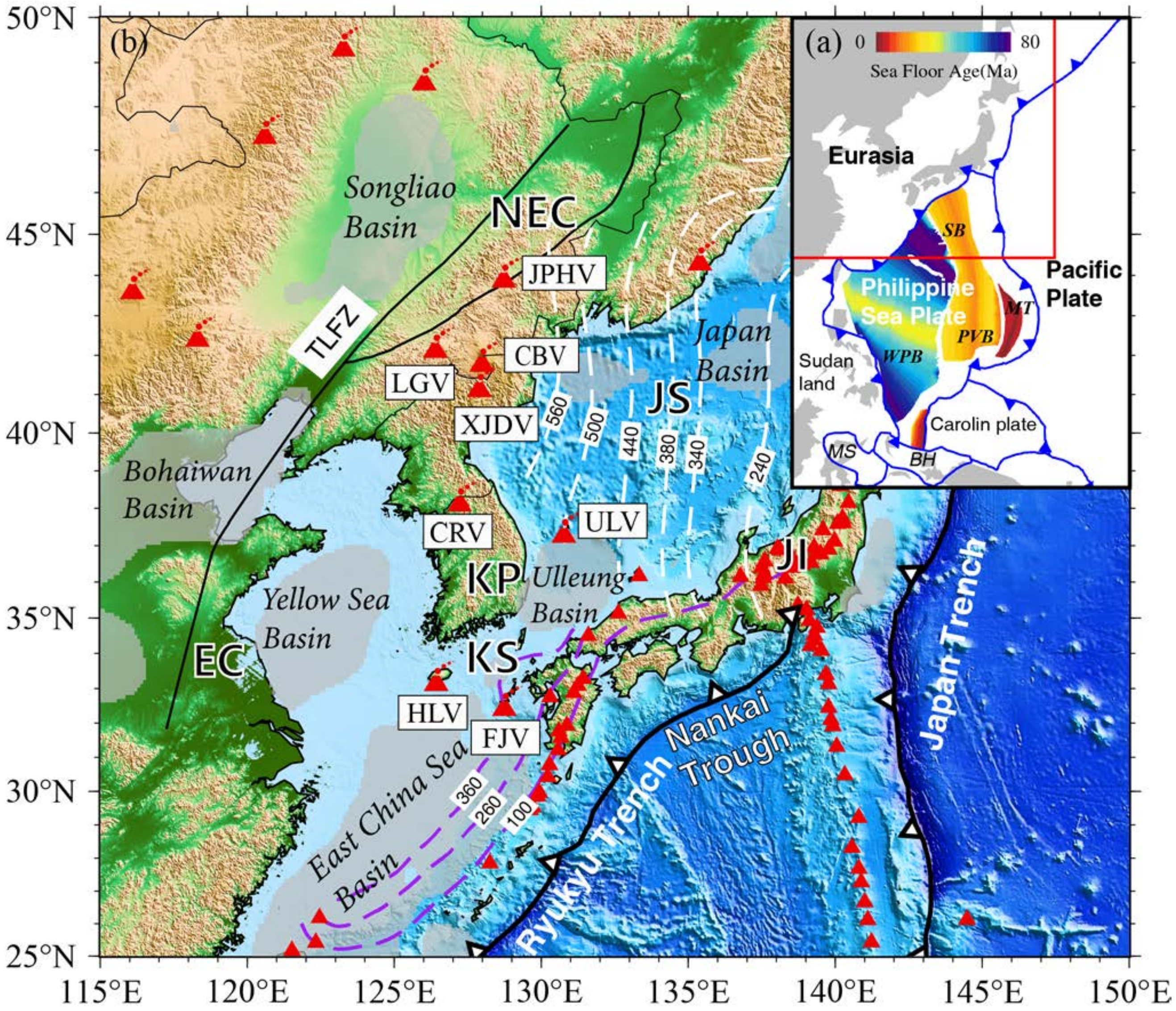

- MS = Molucca Sea minor plate; BH = Bird's Head minor plate; WPB = West Philippine Basin; SB = Shikoku Basin; PVB = Parece Vela Basin; MT = Mariana Trough.
- NEC = northeast China; ENCC=Eastern North Chian Craton ; KP = Korean Peninsula; KS = Korea Strait; SoJ = Sea of Japan; JI = Japanese Island.
- CBV = Changbaishan volcano; JPHV = Jingpohu volcano; LGV = Longgang volcano; XJDV = Xianjingdao volcano; CRV = Chuga-Ryong volcano; ULV = Ulleung volcano; HLV = Halla volcano; FJV = Fukue-jima volcano. TLFZ =Tanlu fault zone

Background

- Questions about intraplate volcanoes
  - ➢ How is the large-scale mantle upwelling related to specific volcanoes?

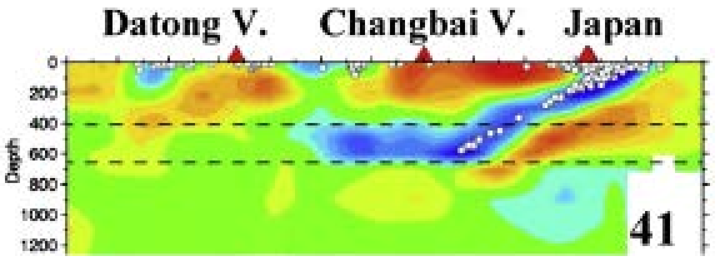

(Zhao et al., 2009)

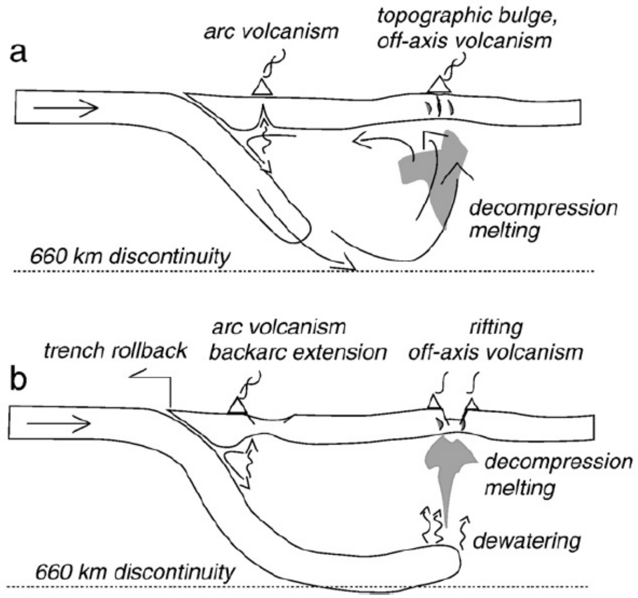

(Faccenna et al., 2010)

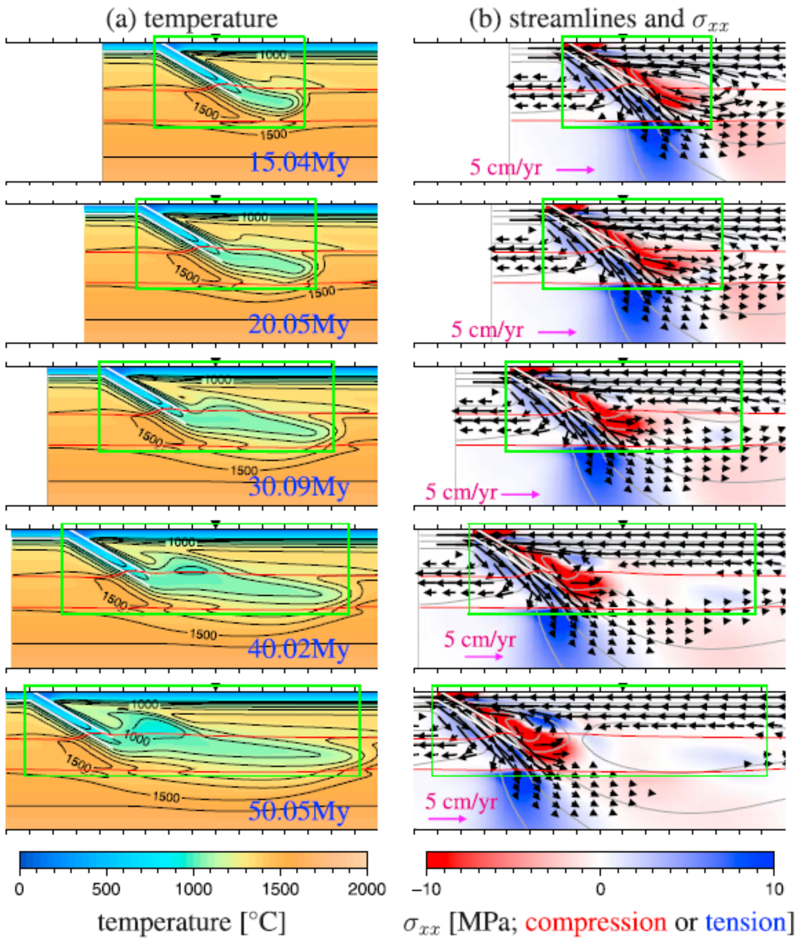

(Kameyama, 2012)

Background

- Questions about geodynamic process reflected in mantle flow
  - What performance ?
  - Controlled by subduction? Back arc extension? Other reason?

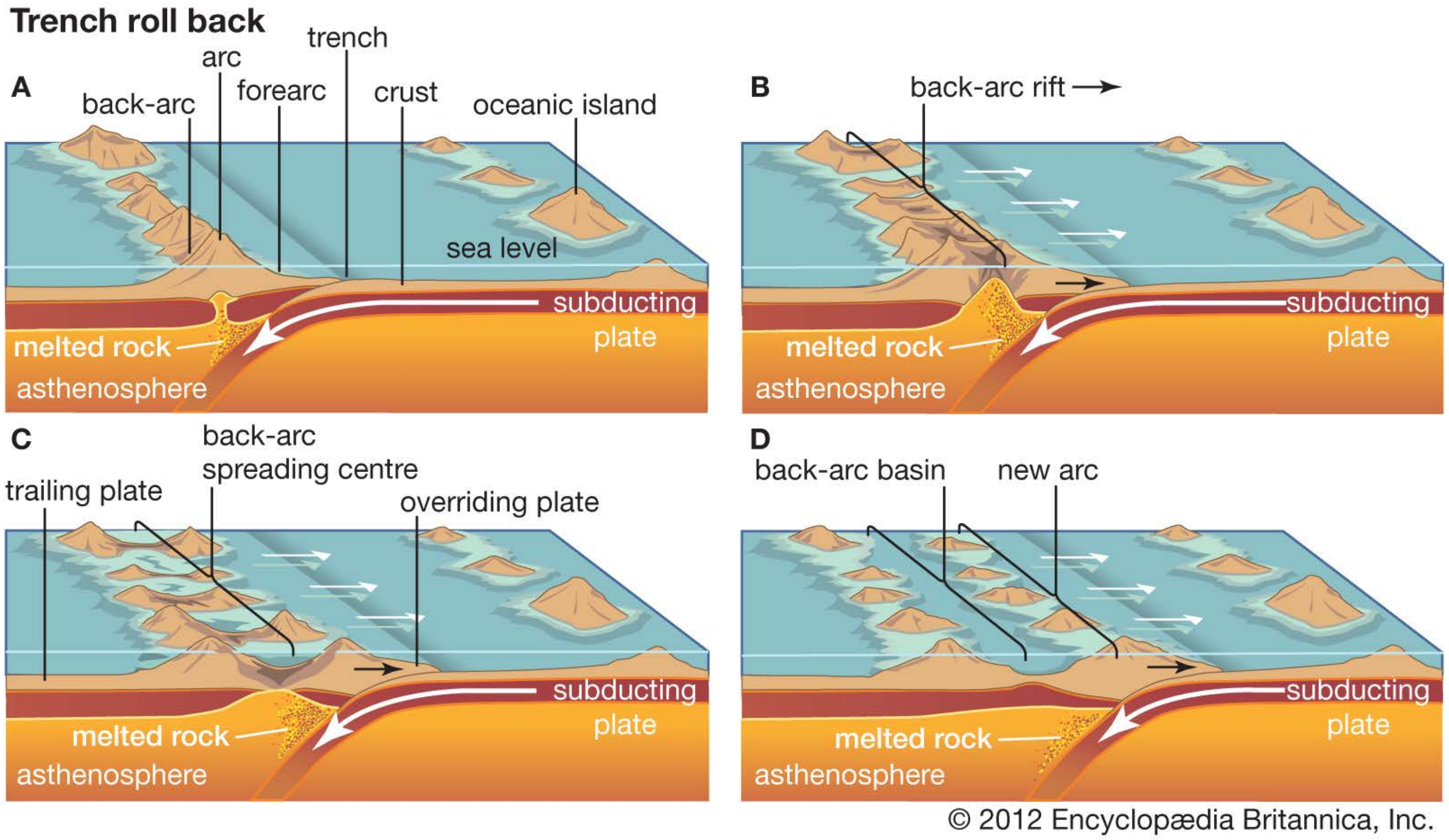

Data and Method

- **Classical representation of Rayleigh-wave and shear wave velocity azimuthal anisotropy**

➢ **For phase velocity:**

Rayleigh wave

$$\boxed{\delta c_R(\omega,\psi) \approx a_0(\omega) + a_c(\omega)\cos 2\psi + a_s(\omega)\sin 2\psi}$$

$$a_{c,s}(\omega) \approx \int_0^H \left(\frac{\partial c_R(\omega)}{\partial A} B_{c,s} + \frac{\partial c_R(\omega)}{\partial L} G_{c,s} \right) dz$$

$$\gamma^{(i)} = \frac{B_{c,s}}{A^{(i)}} \Big/ \frac{G_{c,s}}{L^{(i)}} \qquad \hat{G}_{c,s} = \frac{G_{c,s}}{L}$$

$$a_{c,s}(\omega_j) \approx \Sigma_{i=1}^{K} \left(\gamma^{(i)} A^{(i)} \frac{\delta c_R(\omega_j)}{\delta A^{(i)}} + L^{(i)} \frac{\delta c_R(\omega_j)}{\delta L^{(i)}} \right) \hat{G}_{c,s}^{(i)}$$

Inversion : phase velocity c_R + $a_{c,s}$ ➔ Shear wave velocity V_{SV} + $G_{c,s}\ /L$

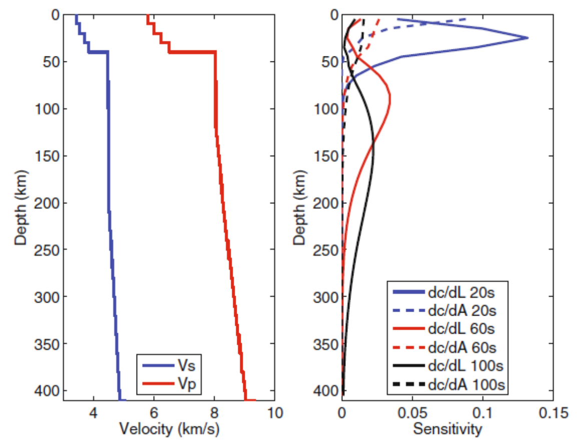

Fig. 1 1-D velocity model (*left*) and its corresponding sensitivity kernels for $\partial c_R/\partial L$ and $\partial c_R/\partial A$ at different periods (*right*)

Sensitivity Kernel (Yao, 2015)

➢ **For shear wave velocity:**

$$\hat{V}_{SV}(\psi) \approx \sqrt{\frac{L + G_c \cos 2\psi + G_s \sin 2\psi}{\rho}}$$

$$\frac{G_{c,s}}{L} \ll 1$$

$$\approx V_{SV}\left(1 + \frac{G_c}{2L}\cos 2\psi + \frac{G_s}{2L}\sin 2\psi\right)$$

$$= V_{SV}(1 + A_{vs}\cos(2\psi - \phi_{vs}))$$

Notice: $|A_{vs}| = 0.5\sqrt{\left(\frac{G_c}{L}\right)^2 + \left(\frac{G_s}{L}\right)^2}$

$$\phi_{vs} = 0.5\arctan(G_s/G_c)$$

Data and Method

- **Previous work: Two-station surface wave tomography** (Fan et al., GRL,2020)

Average dispersion along interstation paths → Phase velocity on all Knots: $c_R(\omega, \psi)$ → Isotropic+Anisotropic Rayleigh wave phase velocity map

gridding parameterization

Data in this study

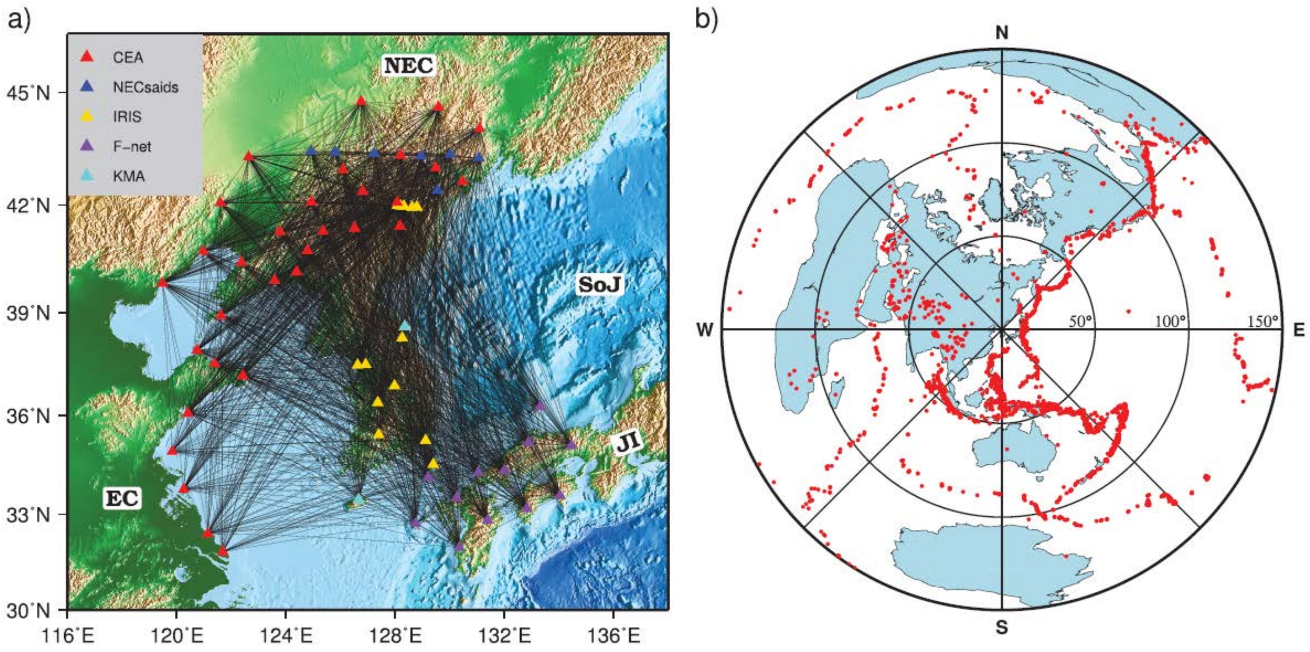

Distribution of stations, ray paths and selected earthquakes (Fan et al., 2020)

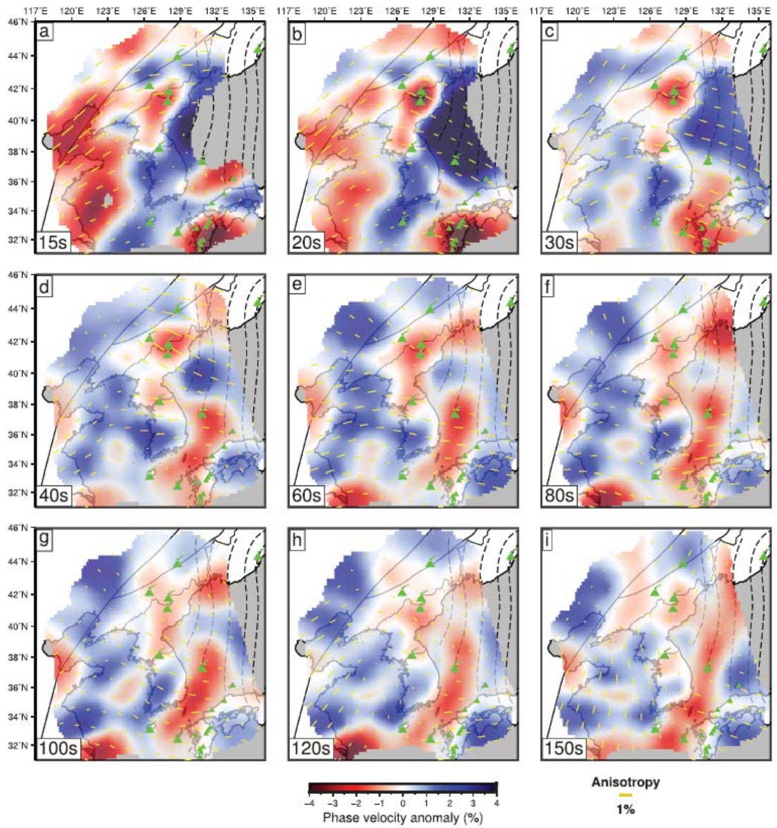

Data and Method

- **reversible jump Markov Chain Monte Carlo**

Bayes theory: $\mathrm{P}(m|d) \propto \mathrm{P}(d|m) \cdot \mathrm{P}(m)$

Model dimension is variable:

- MCMC is **reversible** itself
- Transdimensional sampling ---- "**jumping**" between dimension-different model space

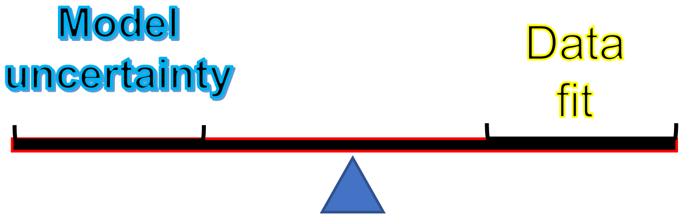

Balance the uncertainty and misfit automatically

Trans-dimensional proposal

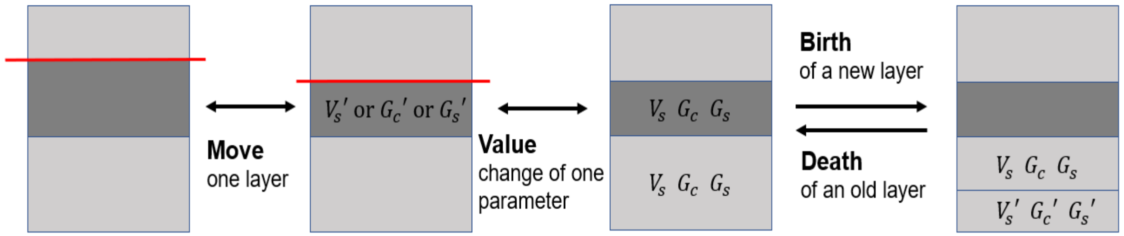

4 types of proposal processes in rj-MCMC algorithm

Simultaneous Inversion:
Shear wave velocity + anisotropy

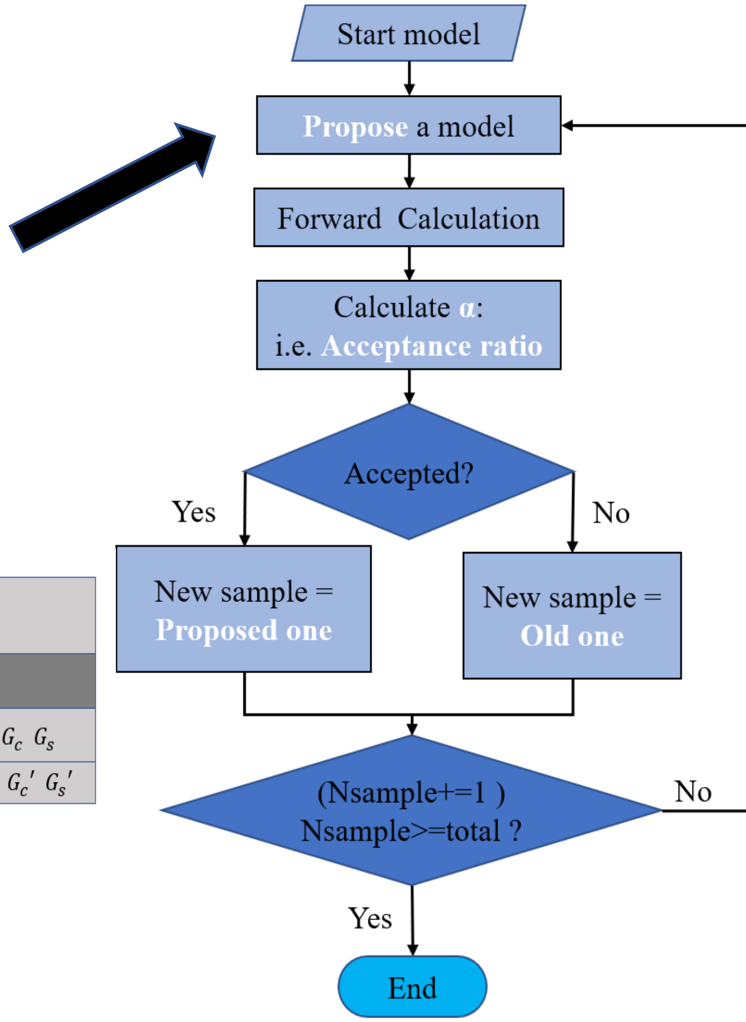

Data and Method

- **Our improvement: Layered prior for Shear wave velocity**

Surface wave: insensitive to discontinuities

Uniform prior? ✕

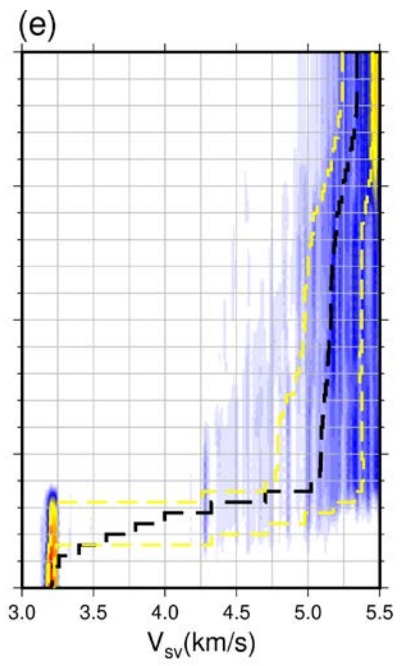

Efficiency ↑
Accuracy ↑

Complex prior √

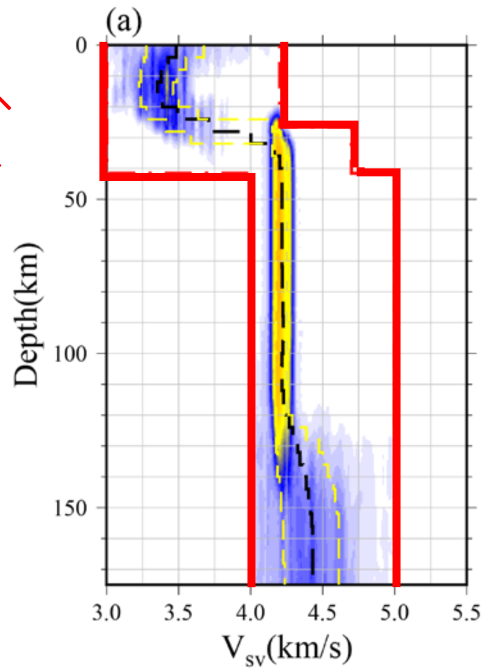

- **Moho:** CRUST1.0±7.5km
- **Vs:** Layered prior setting

Depth	min V_{sv} (km/s)	max V_{sv} (km/s)
0~min Moho	3.0	4.2
In Moho Range	3.5	4.7
max Moho~300km	4.0	5.0
300~400km	4.0	5.5

Results and Discussion

1. Single Knot

Data fit

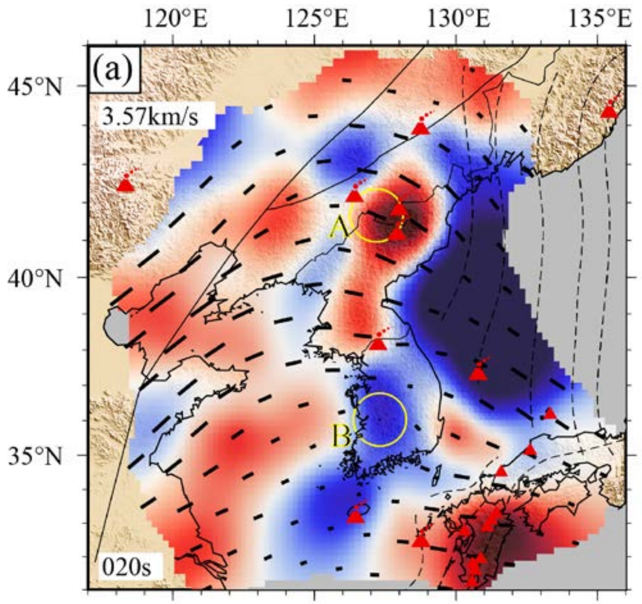

A: near Changbaishan Volcano

B: near high-velocity block of SW Korean Peninsula

cR

ac

as

Example A

Example B

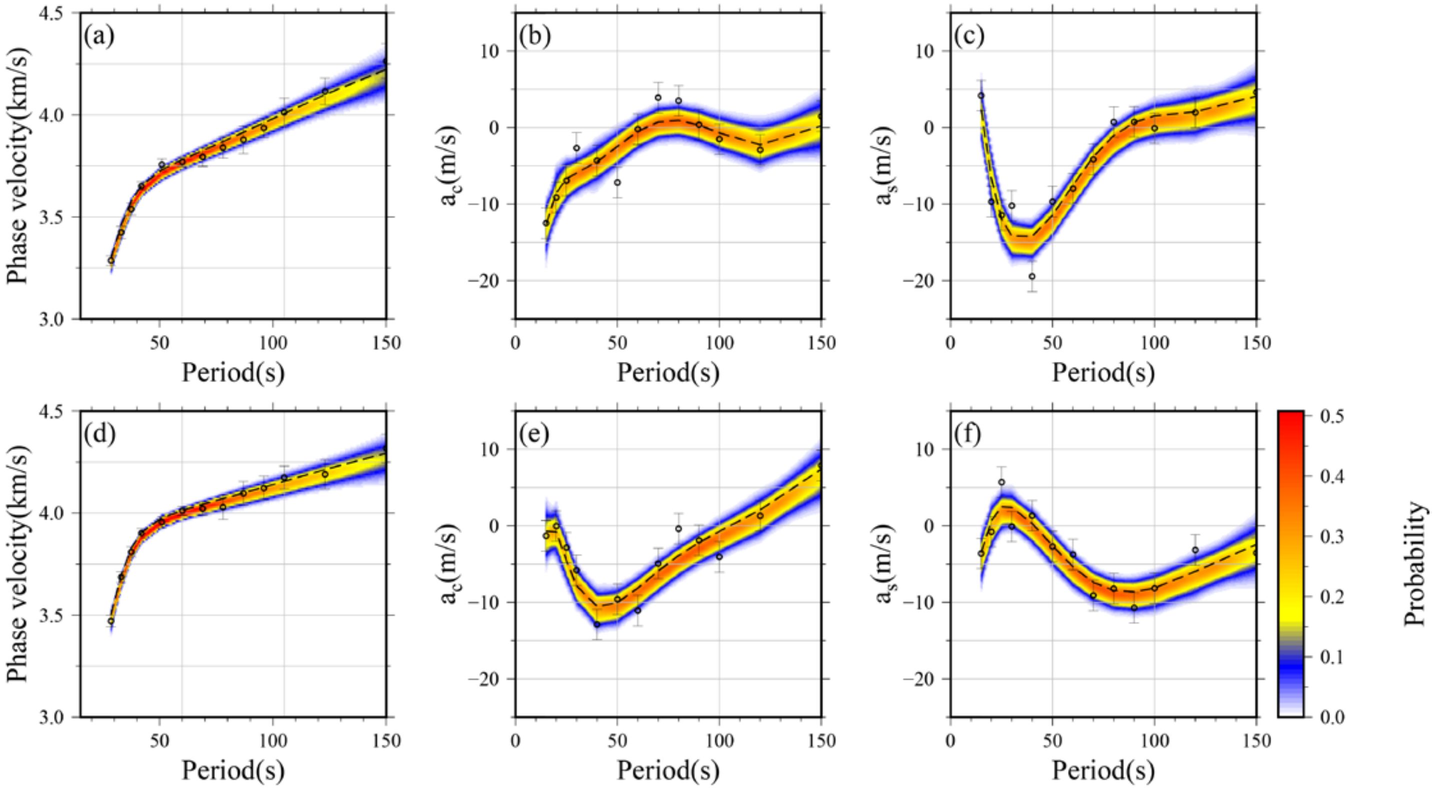

Results and Discussion

1. Single Knot

Model result

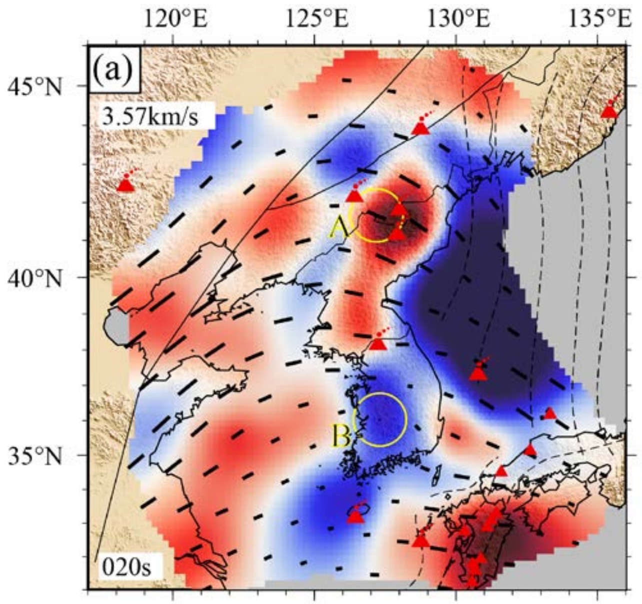

A: near Changbaishan Volcano

B: near high-velocity block of SW Korean Peninsula

Example A

Example B

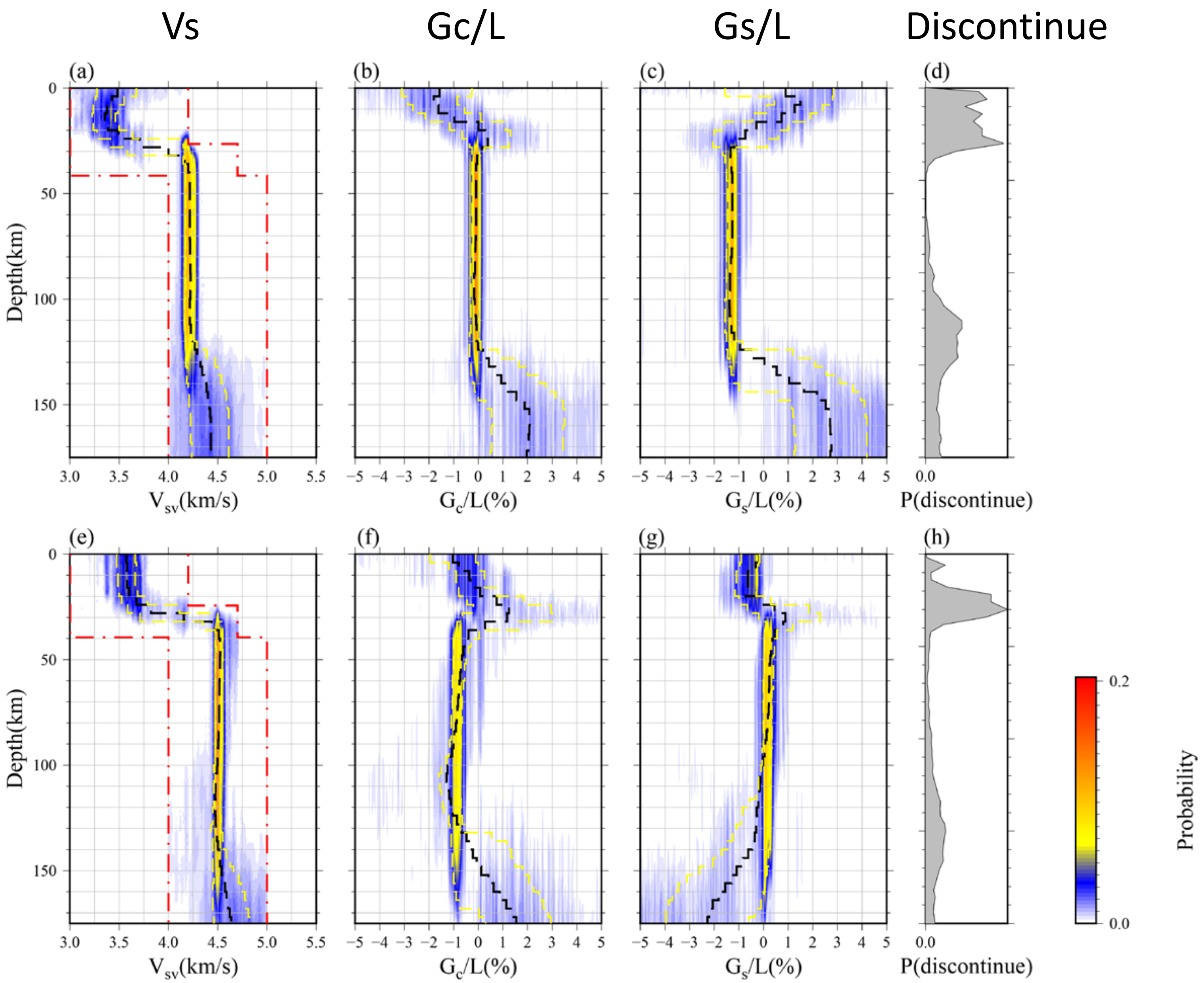

2. 3-D model

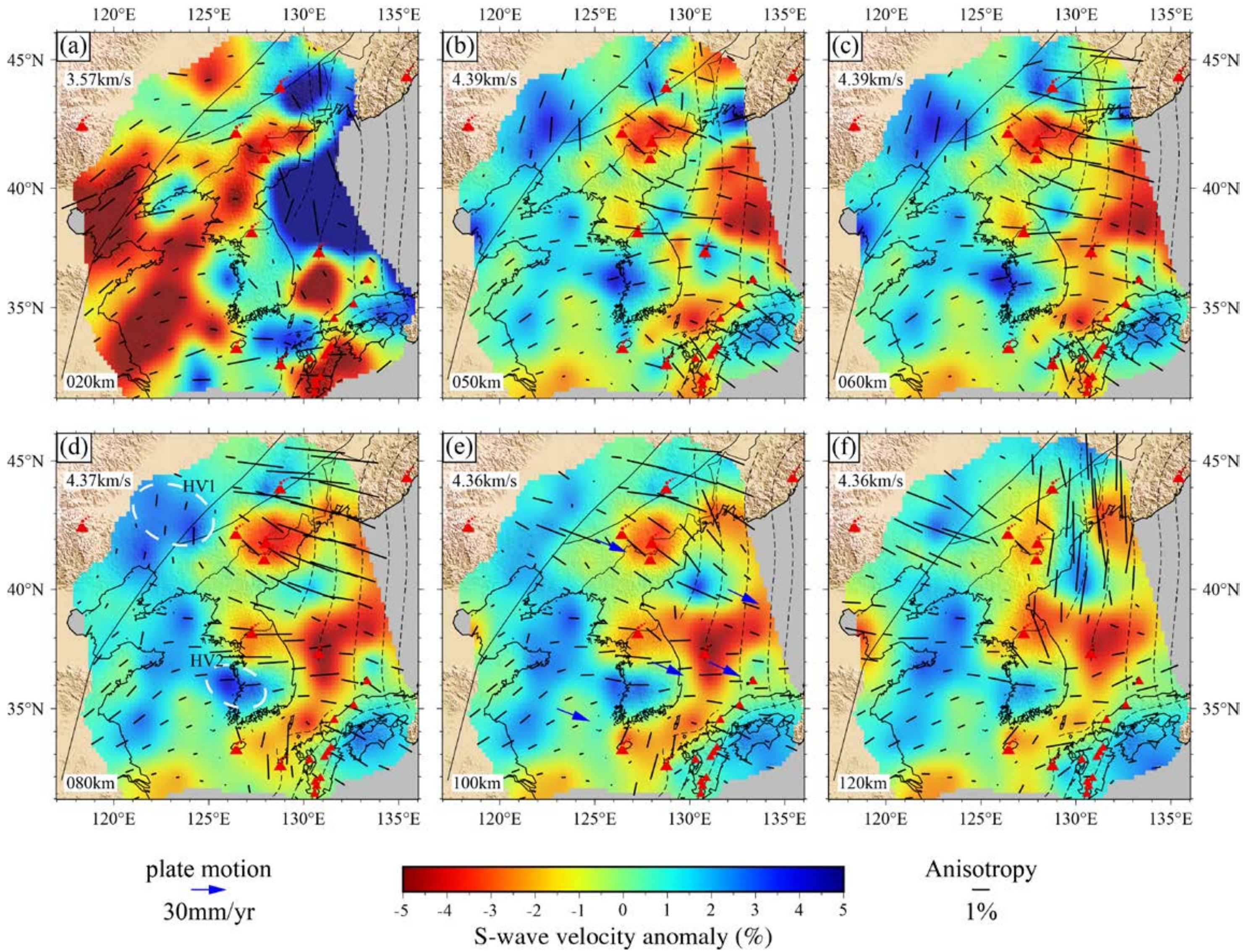

Horizontal slices at different depths

Results and Discussion

2. 3-D model

Point 1: About Intraplate Volcanoes

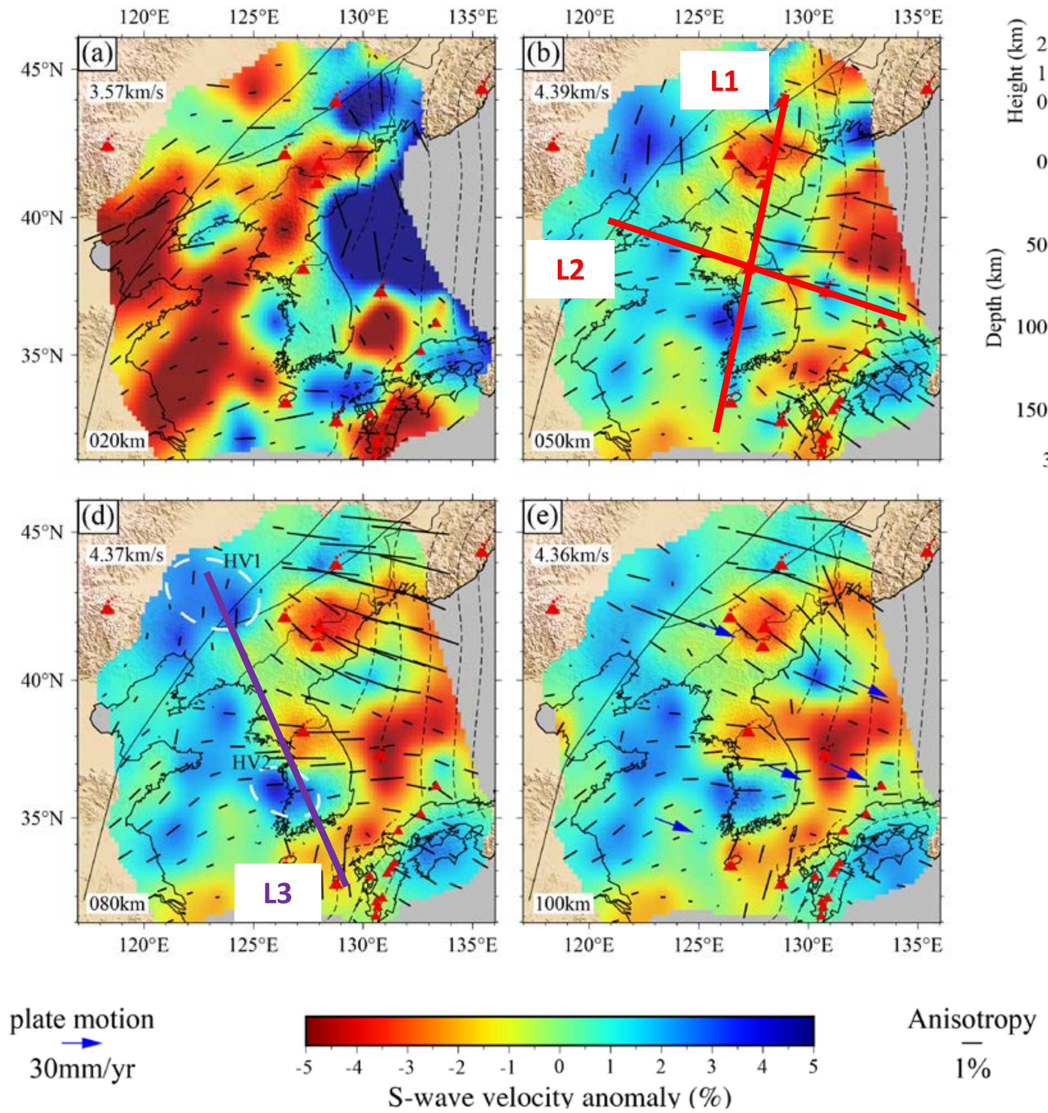

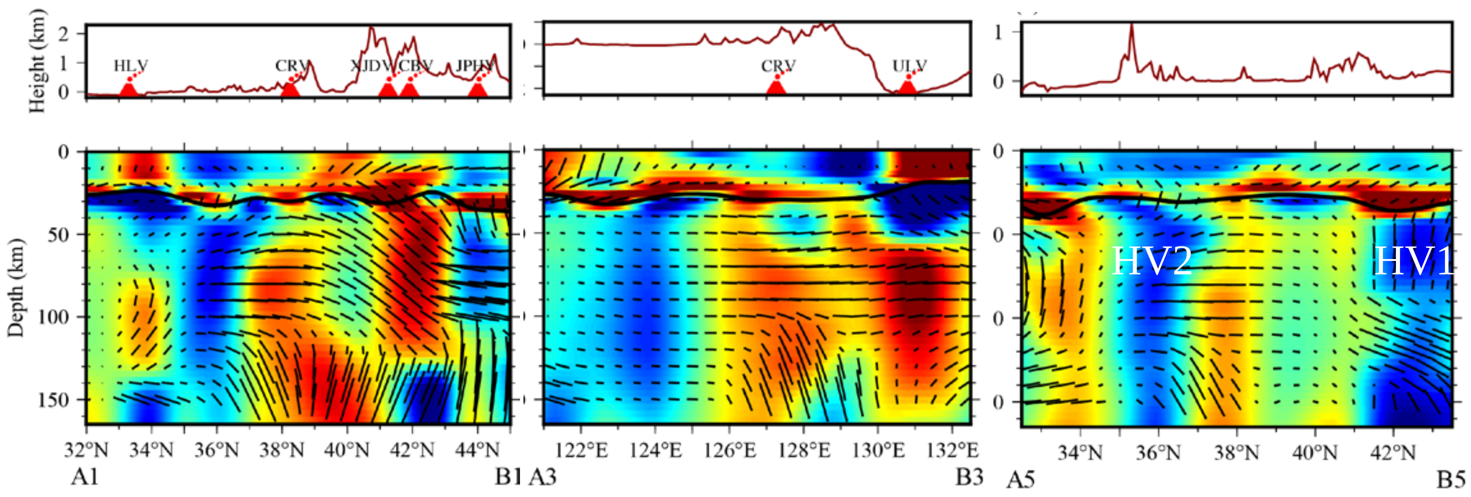

L1 L2 L3

low-velocity area:

- Beneath volcanoes
- Localized

high-velocity block:

- Extending to ~150km
- Near volcanoes

2. 3-D model

Point 1: About Intraplate Volcanoes

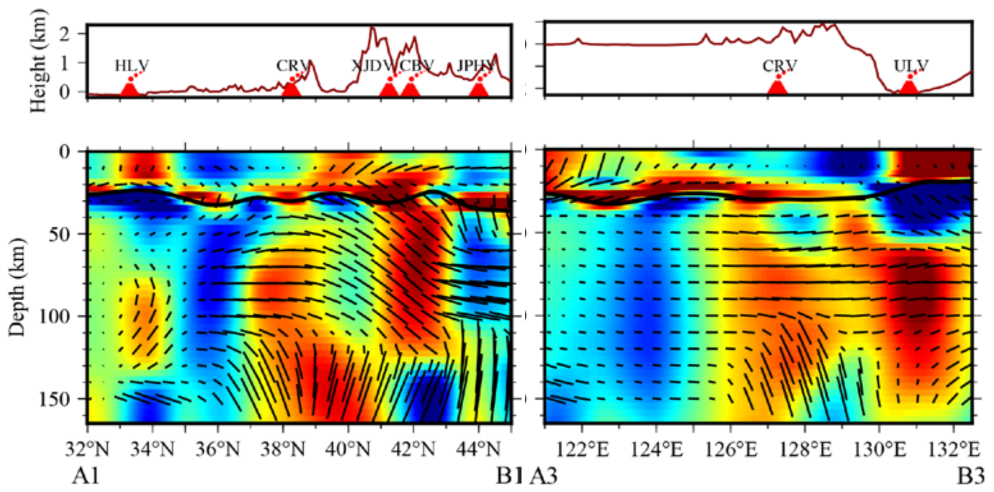

L1 L2

- Localized low-velocity related to deeper upwellings

The upwelling from deeper mantle of big mantle wedge display a characteristic of localized low-velocity area at the uppermost mantle

Results and Discussion

2. 3-D model

Point 1: About Intraplate Volcanoes

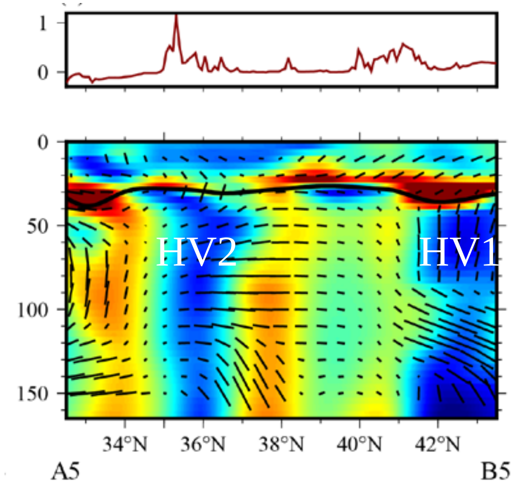

L3

Lithospheric block to ~150km

HV1:

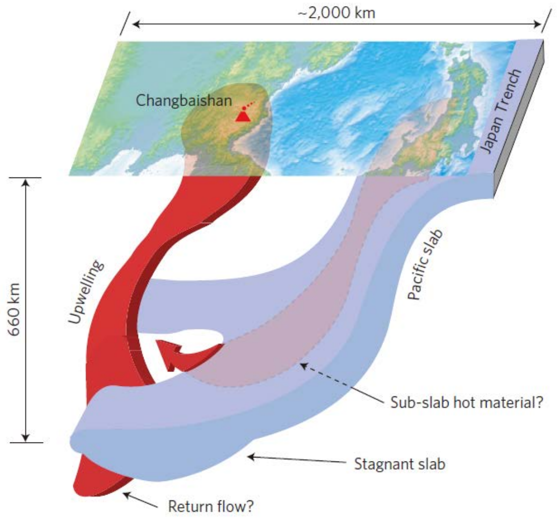

（Tang et al., 2014）

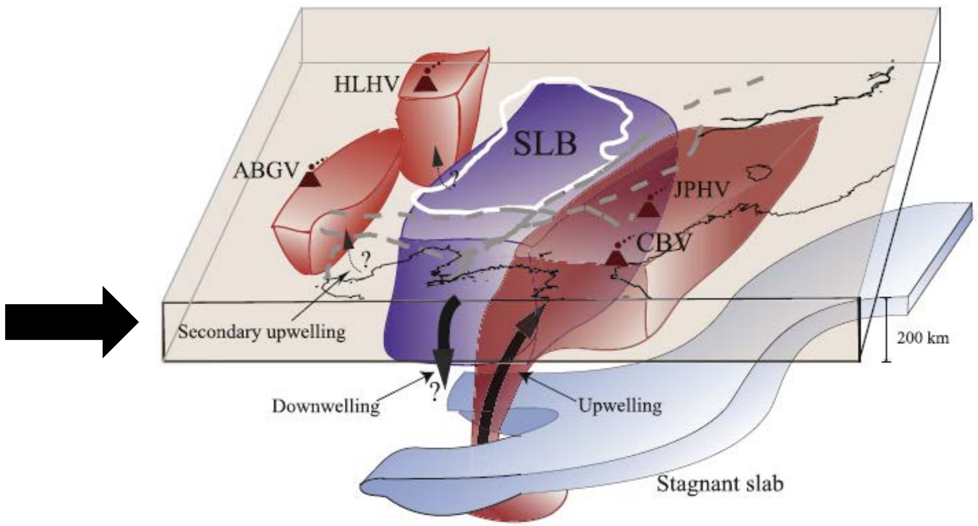

（Guo et al., 2016）

- NE China, Supporting:

Downwelling of Songliao Basin, inducing localized convective upwelling induced by

2. 3-D model

Point 1: About Intraplate Volcanoes

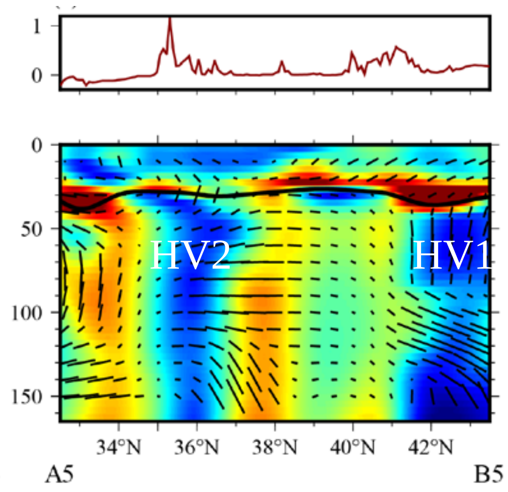

L3

Lithospheric block to ~150km

HV2:

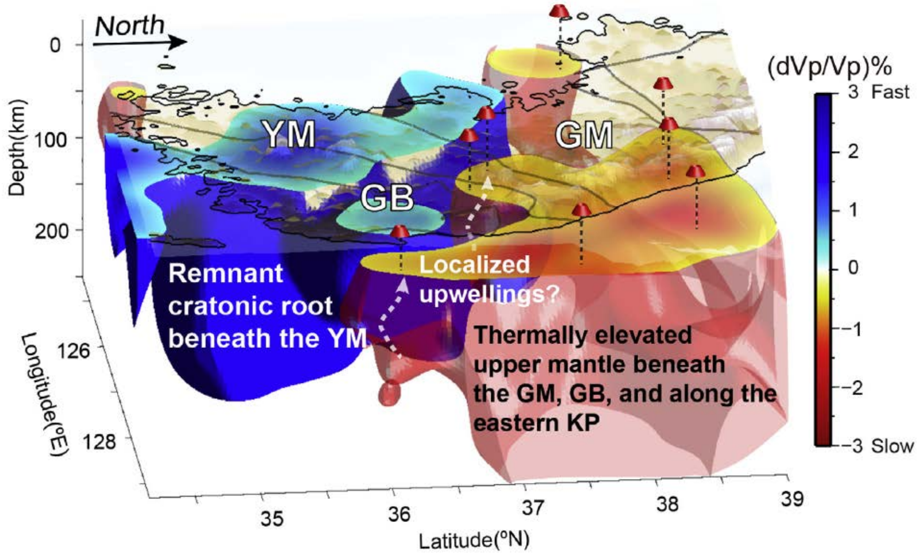

(Song et al., 2020)

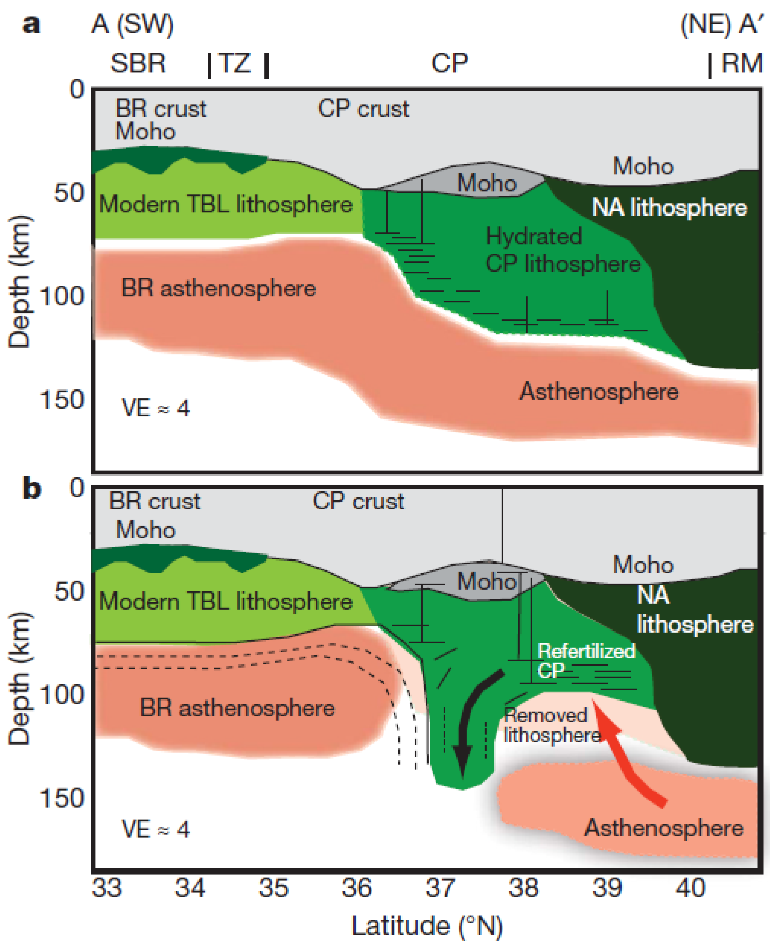

Delamination-style convective lithospheric downwelling in the Colorado Plateau (Levander. et al, 2011)

- SW Korean :
  - Possible cratonic root
  - Possible process of lthospheric dripping and convective upwelling

2. 3-D model

Point 2: About Mantle Flow (two-layer model)

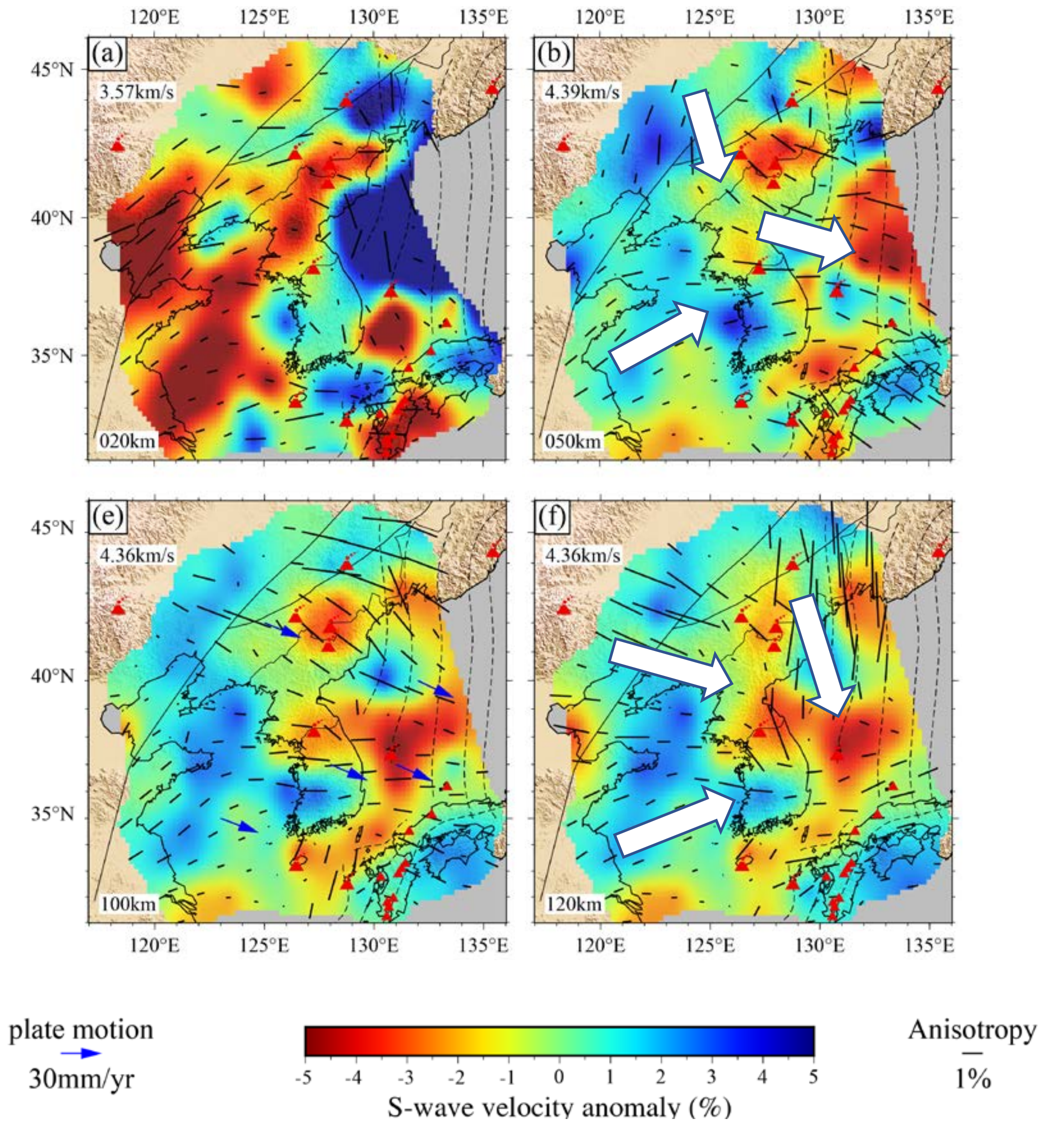

- Upper layer: perpendicular to the Pacific slab

Possibly Controlled by Pacific subduction and back arc extension

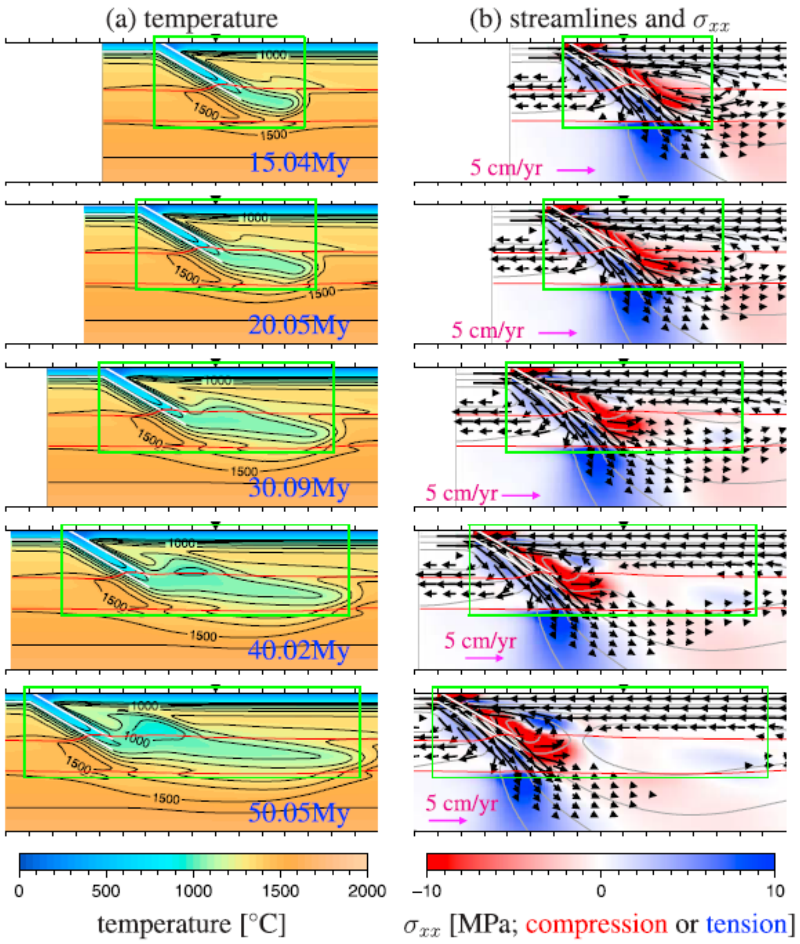

(Kameyama, 2012)

Results and Discussion

2. 3-D model

Point 2: About Mantle Flow (two-layer model)

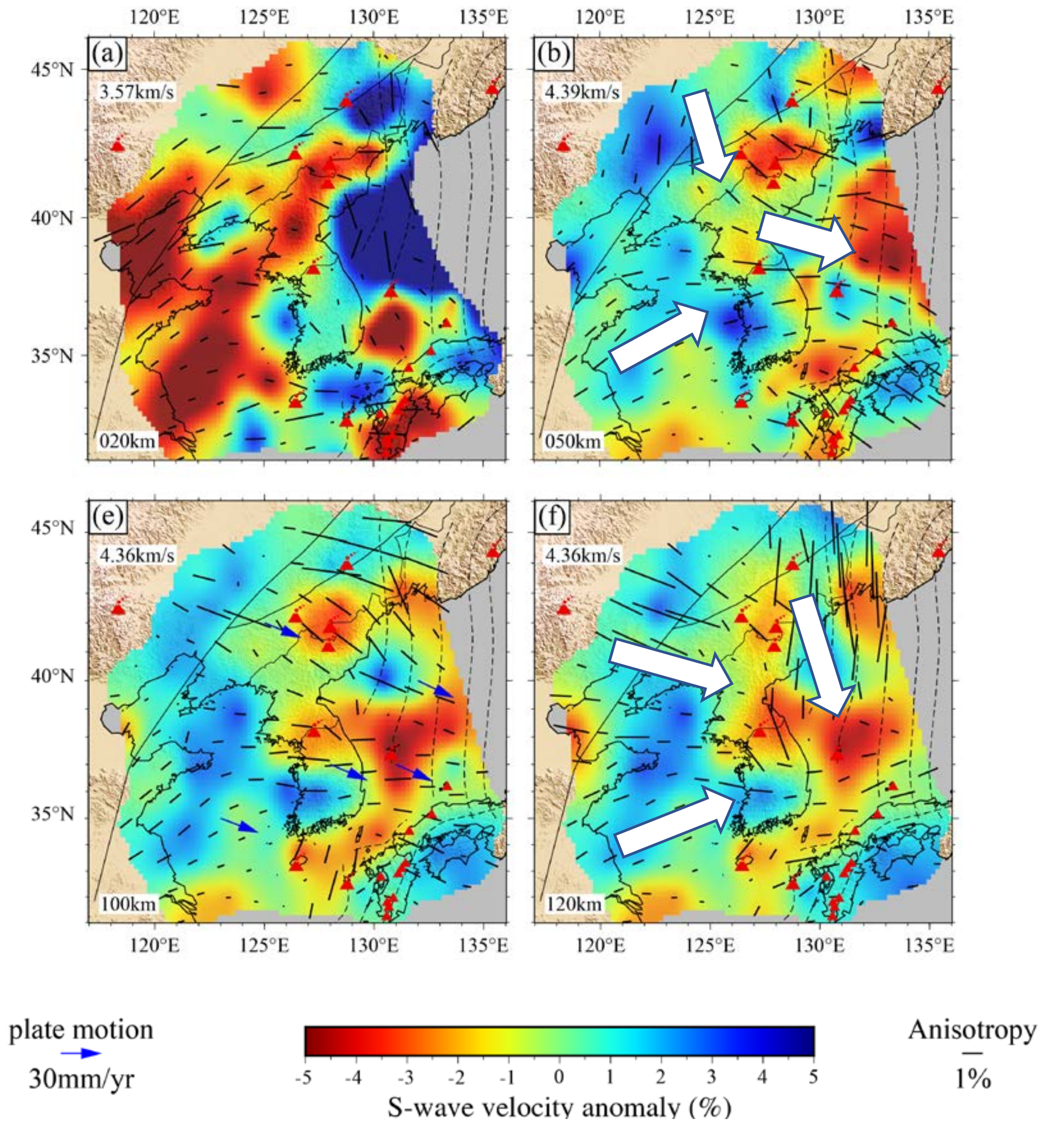

- Lower layer:
  - ➢ Seems to be unrelated to the mantle flow caused by the subduction plate
  - ➢ **Background mantle flow associated with plate movement?**
  - ➢ **Mantle flow caused by other factors?**

Results and Discussion

2. 3-D model

Point 2: About Mantle Flow (two-layer model)

- Two-layer model: SKS check

➢ Prediction based on this model fits well with observations in this region, especially about the fast direction

➢ **A trend converging in SW Japan**

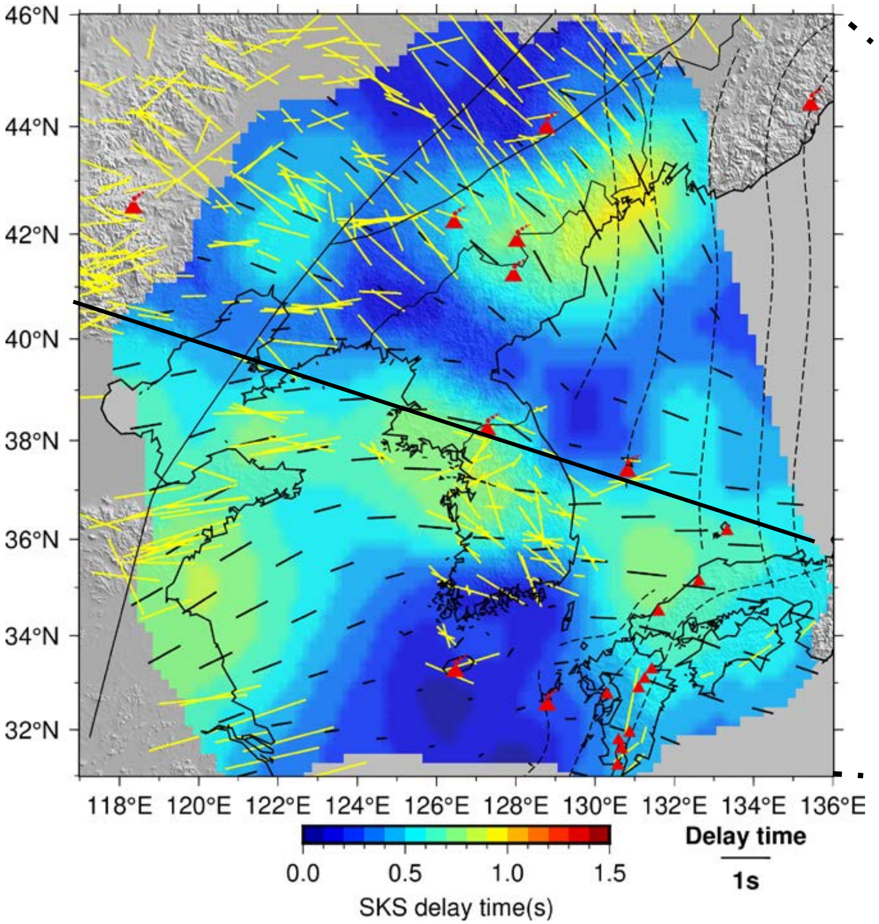

SKS predicted (0~150km)
(Method in Montagner et al., 2000)

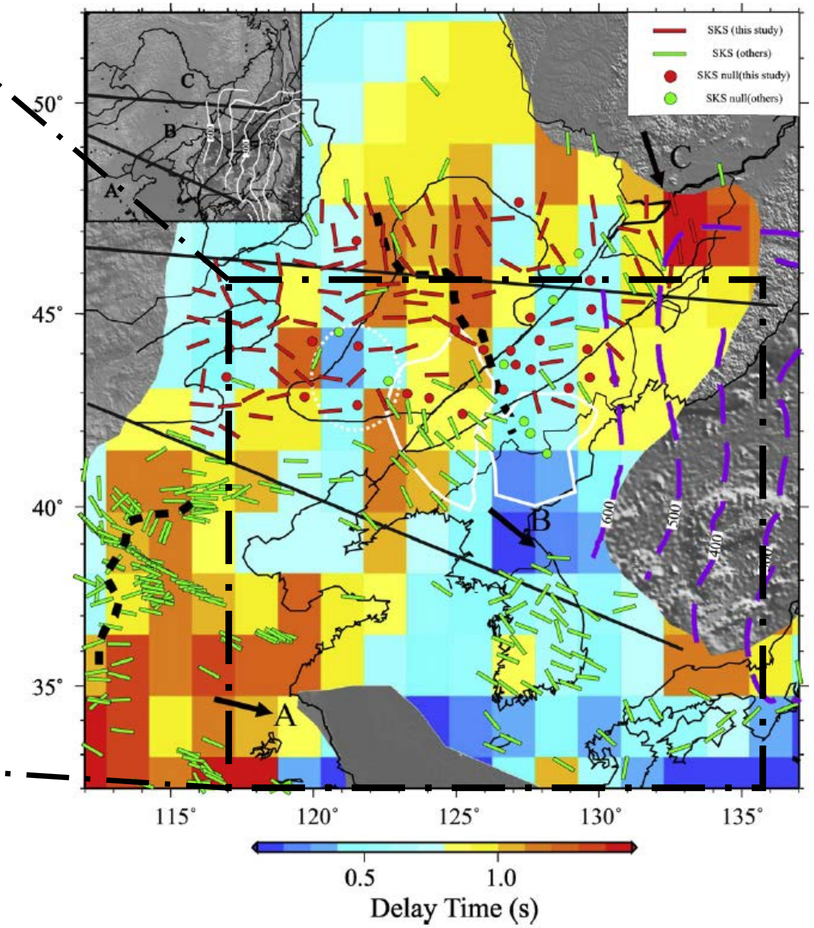

SKS splitting results (Summarized by Li et al., 2017)

Results and Discussion

2. 3-D model

Point 2: About Mantle Flow (two-layer model)

- Two-layer model: SKS check

➢ Prediction based on this model fits well with observations in this region, especially about the fast direction

➢ **A trend converging in SW Japan**

Possible mantle flow across the Nankai through caused by the expansion of Philippine Sea Plate (See background)

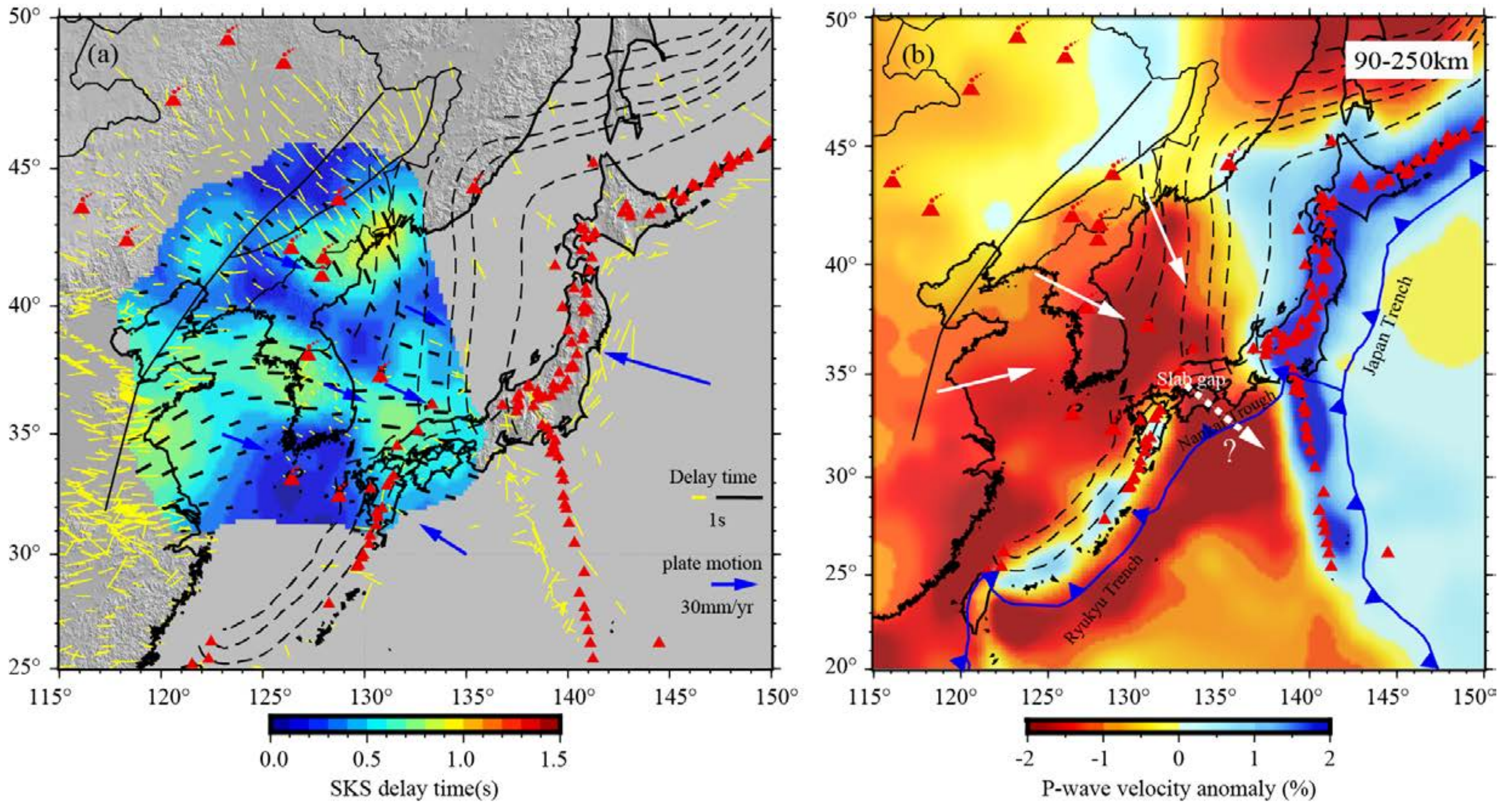

Yellow bar: observation
Black bar: prediction of our model

P-wave model: GAP-P4
(Obayashi et al., 2013)

Conclusion

- About the rj-MCMC method

  - Good distribution can be obtained through rj-MCMC inversion. The efficiency and reliability of inversion can be greatly improved when adding the layered prior

- About the intraplate volcanism

  - localized upwelling with lateral connections between volcanoes can be observed in uppermost mantle, apart from upwelling in the whole big mantle wedge from deeper mantle

  - Convective local upwelling induced by lithospheric dripping may exist in South Korea

- About the anisotropy and related dynamical feature

  - Apparent anisotropy related to back-arc extension can be found beneath the Japan Sea

  - Two-layer anisotropy can be observed in this region. The predicted SKS splitting patterns based on it fit well with the observations, showing more complex mechanism of mantle flow.

  - The anisotropy pattern with a trend converging in SW Japan may be related to ossible mantle flow across the Nankai through caused by the expansion of Philippine Sea Plate (See background)

Reference

Faccenna, C., Becker, T.W., Lallemand, S., Lagabrielle, Y., Funiciello, F., and Piromallo, C. (2010). Subduction-triggered magmatic pulses: A new class of plumes? *Earth and Planetary Science Letters*, 299(1):54–68.

Fan, X., Chen, Q.-F., Legendre, C. P., and Guo, Z. (2020). Intraplate volcanism and regional geodynamics in ne asia revealed by anisotropic rayleigh-wave tomography. *Geophysical Research Letters*, 47(1).

Guo, Z., Chen, Y. J., Ning, J., Yang, Y., Afonso, J. C., and Tang, Y. (2016). Seismic evidence of ongoing sublithosphere upper mantle convection for intra-plate volcanism in northeast china. *Earth and Planetary Science Letters*, 433:31–43.

Kameyama, M. and Nishioka, R. (2012). Generation of ascending flows in the big mantle wedge (bmw) beneath northeast asia induced by retreat and stagnation of subducted slab. *Geophysical Research Letters*, 39(10).

Kreemer, C., W.E. Holt, and A.J. Haines (2003), An integrated global model of present-day plate motions and plate boundary deformation. *Geophys. J. Int.*, 154: 8-34.

Levander, A., Schmandt, B., Miller, M. S., Liu, K., Karlstrom, K. E., Crow, R. S., Lee, C. T. A., and Humphreys, E. D. (2011). Continuing colorado plateau uplift by delamination-style convective lithospheric downwelling. *Nature*, 472(7344):461–U540.

Montagner, J.-P., Griot-Pommera, D.-A., and Lavé, J. (2000). How to relate body wave and surface wave anisotropy? *Journal of Geophysical Research: Solid Earth*, 105(B8):19015–19027.

Reference

Obayashi, M., Yoshimitsu, J., Nolet, G., Fukao, Y., Shiobara, H., Sugioka, H., Miyamachi, H., and Gao, Y. (2013), Finite frequency whole mantle P wave tomography: Improvement of subducted slab images. *Geophys. Res. Lett.*, 40, 5652– 5657.

Seton, M., Müller, R. D., Zahirovic, S., Williams, S., Wright, N., Cannon, J., Whittaker, J., Matthews, K., McGirr, R. (2020), A global dataset of present-day oceanic crustal age and seafloor spreading parameters, *Geochemistry, Geophysics, Geosystems*, doi: 10.1029/2020GC009214

Song, J.-H., Kim, S., and Rhie, J. (2020). Heterogeneous modification and reactivation of a craton margin beneath the korean peninsula from teleseismic travel time tomography. *Gondwana Research*, 81:475–489.

Tang, Y., Obayashi, M., Niu, F., Grand, S. P., Chen, Y. J., Kawakatsu, H., Tanaka, S., Ning, J., and Ni, J. F. (2014). Changbaishan volcanism in northeast china linked to subduction-induced mantle upwelling. *Nature Geoscience*, 7(6):470–475.

Yao, H. (2015). A method for inversion of layered shear wavespeed azimuthal anisotropy from rayleigh wave dispersion using the neighborhood algorithm. *Earthquake Science*, 28(1):59–69.

Zhao, D. and Ohtani, E. (2009). Deep slab subduction and dehydration and their geodynamic consequences: Evidence from seismology and mineral physics. *Gondwana Research*, 16(3):401–413.

Thanks!

e-mail: zzyzpku@pku.edu.cn